The inclusive decay $b \to c\bar{c}s$ revisited

Fabian Krinner[a], Alexander Lenz[b,c], Thomas Rauh[a]

[a] *Physik-Department, Technische Universität München, James-Franck-Straße, 85748 Garching, Germany*
[b] *Institute for Particle Physics and Phenomenology, Durham University, Durham DH1 3LE, UK*
[c] *CERN - Theory Division, PH-TH, Case C01600, CH-1211 Geneva 23*

Abstract

The inclusive decay rate $b \to c\bar{c}s$ is enhanced considerably due to perturbative QCD corrections. We recalculate the dominant part of the NLO-QCD corrections, because they cannot be reconstructed from the literature and we give the full expressions in this paper. Further we include some previously neglected corrections originating from penguin diagrams. Combined with the impressive progress in the accurate determination of input parameters like charm quark mass, bottom quark mass and CKM parameters, this enables us to make a very precise prediction of the corresponding branching ratio $\mathcal{B}(b \to c\bar{c}s) = (23 \pm 2)\%$. This result is an essential ingredient for a model and even decay channel independent search for new physics effects in B decays.

Keywords: B decay, semileptonic branching ratio, charm multiplicity, search for new physics

1. Introduction

Despite the impressive experimental achievements in flavour physics in recent years we still do not have compelling proof for new physics effects. Time by time interesting evidence for deviations has shown up (see e.g. the status of new physics searches in B-mixing in 2010 [1]). Unfortunately most of it vanished as soon as more precise data became available (see e.g. the status of new physics searches in B-mixing in 2012 [2]). Currently the standard model [3, 4, 5] and the CKM mechanism [6, 7] seem to work at an unexpectedly precise level, see e.g. [8, 9] for standard model fits after the Higgs boson [10, 11, 12] discovery [13, 14] .

Nevertheless most of the motivations for looking for an extension of the standard model still remain valid, e.g. an explanation of the baryon asymmetry in the universe or the nature of dark matter. Flavour physics is a mandatory ingredient in the programme of searching for and investigating extensions of the standard model. Finding statistical significant deviations of measurements from the corresponding standard model predictions might provide the first evidence of new physics effects. But even if new physics is detected in other fields, like a direct production of new degrees of freedom at the LHC, then flavour physics will be very helpful in pinning down the properties of the new particles. Finally also in the worst case of finding no direct evidence of beyond standard model physics in the near future, the parameter space of hypothetical new physics models can be shrunk considerably, some models might even be excluded, as it recently happened for the case of a perturbative fourth generation of chiral fermions, see e.g. [8, 15, 16, 17]. One essential prerequisite for all this tasks is clearly the theoretical control of our standard model predictions. Besides the already mentioned fact that there are no huge new physics effects around the corner, we learnt from the LHC data a lot about our theoretical tools. The applicability of the Heavy-Quark-Expansion (HQE) [18, 19, 20, 21, 22, 23, 24, 25] was questioned many times in the literature, in particular for decays with a limited phase space in the final states, e.g. decays like $b \to c\bar{c}s$. see e.g. [26, 27, 28] . Thus, an ideal testing ground for the HQE is the decay rate difference $\Delta\Gamma_s$ of the neutral B_s mesons. The dominant contribution to this quantity is given by the decay channels $\bar{B}_s \to D_s^{(*)+} D_s^{(*)-}$ [29, 30] (triggered by the quark level decay $b \to c\bar{c}s$), with an energy release of only about 1.4 GeV. If the HQE does not converge, because of a too large expansion parameter (1/energy release) then this should clearly show up in $\Delta\Gamma_s$. In 2012 LHCb made the first measurement (more than five standard deviations from zero) of the decay rate difference by investigating the decay $B_s \to J/\psi\phi$ [31], see [32] for the previously published result. $\Delta\Gamma_s$ was also studied by the ATLAS Collaboration [33][1], the CDF Collaboration [34] and the D0 Collaboration [35] and the values from LHCb were recently updated at Moriond 2013 [36]. The Heavy Flavour Averaging Group (HFAG) [37] gives as an average the value

$$\Delta\Gamma_s^{Exp.} = +0.081 \pm 0.011 \text{ ps}^{-1} , \tag{1}$$

[1]ATLAS presented a flavour tagged update of this result at BEAUTY 2013.

which excellently agrees with the standard model prediction [38][2]

$$\Delta\Gamma_s^{SM} = +0.087 \pm 0.021 \text{ ps}^{-1} . \tag{2}$$

This clearly shows the validity of the HQE, in particular also for the mistrusted decay channel $b \to c\bar{c}s$, see [44] for a more detailed discussion. There are also some indications that the HQE might even work in the charm sector when applied to the lifetimes of D mesons, see [45] for a very recent investigation.

Another important aspect of the new experimental results is the fact, that there is still plenty of room for NP effects. In B_s-mixing we still could have new phases which are considerably larger than the standard model phases [2]. Also the investigation of rare decays still leaves quite some sizable room for beyond standard model effects, see e.g. [46, 47, 48] for some very recent constraints.

To summarise the current situation (see also [49] for a review): the desired huge new physics effects have not been found, but there is still room for some sizable effects. In order to disentangle such effects higher precision is mandatory both in experiment and theory. In that respect it is of course very promising that our theoretical tools have passed many non-trivial tests.

In this paper we provide some theoretical prerequisites for a model independent and even decay channel independent search of new physics. We propose a re-investigation of inclusive b-decays.

Motivated by the experimental measurement of the dimuon asymmetry A_{sl}^b from the D0 collaboration at Tevatron in 2010 [50, 51] and 2011 [52], which differs by 3.9 standard deviations from the standard model prediction given in [39][3] it became quite popular to investigate new physics models that enhance the absorptive part of the B_d and B_s mixing amplitudes. Such an enhancement would also lead to considerable modifications of different B-meson decay channels. One promising candidate was the decay $B_s \to \tau^+\tau^-$, which was investigated e.g. in [53, 54, 55, 56, 57, 58]. Having stronger experimental bounds on this channel would be very helpful, even if the significance of the deviation in the dimuon asymmetry went down recently [59].

A large branching ratio for $B_s \to \tau^+\tau^-$ would also affect several inclusive

[2]This prediction is based on the NLO-QCD calculations in [39, 40, 41, 42]; most of these results were confirmed in [43].

[3]This prediction is based on the NLO-QCD calculations in [40, 41, 42]; these results were confirmed in [43].

decay rates: the total decay rate $\Gamma_{tot} = 1/\tau$, the charm-less decay rate $\Gamma(b \to \text{no charm})$, the semileptonic branching ratio $B_{sl} = \Gamma_{sl}/\Gamma_{tot}$ and the average number of charm quarks per b-decay n_c. Some time ago these quantities received quite some attention, see e.g. [60, 61, 26, 62, 63, 64, 65, 28, 66, 67, 68, 69] because there seemed to be some discrepancies between theory and experiment. For the investigation of the inclusive branching ratios the NLO-QCD corrections turned out to be very important (see e.g. [70]), they were determined for $b \to cl^-\bar{\nu}$ analytically in [71], for $b \to c\bar{u}d$ in [72], for $b \to c\bar{c}s$ in [73], for $b \to$ no charm in [74] and for $b \to sg$ in [75, 76]. Since the above listed numerical analyses are at least 15 years old and there was a lot of progress in the precise determination of the relevant standard model parameters like CKM elements and quark masses an update of the numerical predictions for inclusive decay rates is clearly overdue. This case is strengthened by the experimental confirmation of the HQE. Moreover an investigation of the inclusive branching ratios is not limited to a certain decay channel like $B_s \to \tau^+\tau^-$, but it is sensitive to all possible decay rates, even if there would be some invisible decay channels. Finally the most recent experimental number for n_c stems from BaBar from 2006 using about $231 \cdot 10^6$ $B\bar{B}$ events [77]. Here clearly an experimental update is possible and also Belle as well as LHCb might investigate these quantities.
Preparing a theoretical update we found, however, that the formulae given in the paper [73] for the $b \to c\bar{c}s$ decay rate give IR divergent expressions. Thus we recalculate these important corrections in this work and include also previously neglected contributions. Comparing our numerical results (for the old input parameters) with the ones given in [73] we find an exact agreement. Hence, we conclude that there were simply several misprints in the formulae of [73]. We give here the corrected expressions for $\Gamma(b \to c\bar{c}s)$ and finally we also perform the numerical analysis with up-to-date input parameters.
The paper is structured as follows: In Section 2 we describe in detail the order $\mathcal{O}(\alpha_s)$ calculation of the decay width of the channel $b \to c\bar{c}s$. Besides discussing the diagrams that were already done in [73], we also calculated some previously neglected contributions in Section 2.7 and Section 2.8. Different quark mass schemes are investigated in Section 2.4. In Section 3 we discuss our final result in detail. First we show explicitly the cancellation of the renormalisation scheme dependence in Section 3.1, next we compare our result in detail with [73] in Section 3.2 and point out the misprints in that work. The up-to-date numerical results for the decay rate are presented and discussed in Section 3.4. Finally we conclude in Section 4. Longer analytic

expressions of our calculation are presented in the Appendix.

2. Calculation of the inclusive $b \to c\bar{c}s$ decay width

In this chapter we discuss the calculation of the inclusive $b \to c\bar{c}s$ decay width up to order $\mathcal{O}(\alpha_s)$ in detail, we also include some previously neglected contributions.

2.1. The effective Hamiltonian

The starting point of our calculation is the effective weak Hamiltonian, which can be written as (see e.g. [78] for a review):

$$\mathcal{H}_{\text{eff}} = \frac{G_F}{\sqrt{2}} \left(\xi_c \sum_{i \in \{1,2\}} C_i Q_i - \xi_t \sum_{i \in \{3...6,8\}} C_i Q_i \right), \tag{3}$$

where G_F denotes the Fermi constant, $\xi_q = V_{qb} V_{qs}^*$ represents the CKM-elements, C_i the Wilson coefficients and Q_i the appearing four quark operators. The individual operators are given by:

$$\begin{aligned}
Q_1 &= \bar{c}_\alpha \Gamma_\mu b_\beta \otimes \bar{s}_\beta \Gamma^\mu c_\alpha, \\
Q_2 &= \bar{c}_\alpha \Gamma_\mu b_\alpha \otimes \bar{s}_\beta \Gamma^\mu c_\beta, \\
Q_3 &= \bar{s}_\alpha \Gamma_\mu b_\alpha \otimes \bar{c}_\beta \Gamma^\mu c_\beta, \\
Q_4 &= \bar{s}_\alpha \Gamma_\mu b_\beta \otimes \bar{c}_\beta \Gamma^\mu c_\alpha, \\
Q_5 &= \bar{s}_\alpha \Gamma_\mu b_\alpha \otimes \bar{c}_\beta \Gamma^\mu_+ c_\beta, \\
Q_6 &= \bar{s}_\alpha \Gamma_\mu b_\beta \otimes \bar{c}_\beta \Gamma^\mu_+ c_\alpha, \\
Q_8 &= -\frac{g_s}{8\pi^2} m_b \bar{s}_\alpha \sigma^{\mu\nu} (1+\gamma_5) T^A_{\alpha\beta} b_\beta G^A_{\mu\nu}.
\end{aligned} \tag{4}$$

α and β denote SU(3) colour indices and g_s is the strong coupling-constant. The appearing Dirac-structures are given by $\Gamma^\mu = \gamma^\mu (1-\gamma_5)$, $\Gamma^\mu_+ = \gamma^\mu (1+\gamma_5)$ and $\sigma^{\mu\nu} = i/2[\gamma^\mu, \gamma^\nu]$.
The Wilson coefficients can be expressed as a series in powers of α_s:

$$C_i = C_i^{(0)} + \frac{\alpha_s}{4\pi} C_i^{(1)} + \mathcal{O}\left(\alpha_s^2\right). \tag{5}$$

Note, that throughout this paper it is always understood, that the Wilson-coefficients are evaluated at the renormalisation-scale μ, i.e.: $C_i = C_i(\mu)$. The same holds for the strong coupling constant: $\alpha_s = \alpha_s(\mu)$, if not stated otherwise.

2.2. The inclusive $b \to c\bar{c}s$ decay width

The inclusive decay width for the channel $b \to c\bar{c}s$ is given as a phase space integration over the squared matrix element, describing the transition of the b-quark into the final state $c\bar{c}s$ via the weak Hamiltonian.

$$\Gamma_{c\bar{c}s} = \frac{8\pi^4}{m_b} \int \prod_{i=1}^{3} \left[\frac{d^3 p_i}{(2\pi)^3 2E_i} \right] \delta^{(4)} \left(p_B - \sum_{i=1}^{3} p_i \right) \left| \langle c\bar{c}s | \mathcal{H}_{eff} | b \rangle \right|^2 . \quad (6)$$

The above matrix element can be expanded in powers of the strong coupling

$$\begin{aligned} \mathcal{M} &:= \langle c\bar{c}s | \mathcal{H}_{eff} | b \rangle \\ &= \mathcal{M}^{(0)} + \frac{\alpha_s}{4\pi} \mathcal{M}^{(1)} + \mathcal{O}\left(\frac{\alpha_s}{4\pi} \right)^2 , \end{aligned} \quad (7)$$

thus we get for the squared matrix element

$$|\mathcal{M}|^2 = \mathcal{M}^{(0)\dagger} \mathcal{M}^{(0)} + \frac{\alpha_s}{4\pi} \left(\mathcal{M}^{(0)\dagger} \mathcal{M}^{(1)} + \mathcal{M}^{(1)\dagger} \mathcal{M}^{(0)} \right) + \mathcal{O}\left(\frac{\alpha_s}{4\pi} \right)^2 . \quad (8)$$

Therefore the inclusive decay width for the channel $b \to c\bar{c}s$ can be written as:

$$\Gamma_{c\bar{c}s} = \Gamma_{c\bar{c}s}^{(0)} + \frac{\alpha_s}{4\pi} \Gamma_{c\bar{c}s}^{(1)} + \mathcal{O}\left(\alpha_s^2 \right) , \quad (9)$$

with the leading-order (LO) contribution $\Gamma_{c\bar{c}s}^{(0)}$ and the sizable next-to-leading-order (NLO) correction $\Gamma_{c\bar{c}s}^{(1)}$. The LO decay width is given as:

$$\Gamma_{c\bar{c}s}^{(0)} = \Gamma_0 |\xi_c|^2 g \mathcal{N}_a . \quad (10)$$

The factor Γ_0 is the width of a decay into three mass- and colourless particles:

$$\Gamma_0 = \frac{G_F^2 m_b^5}{192\pi^3} . \quad (11)$$

The factor $\mathcal{N}_a$ stems from the leading term in Eq.(8), it is a linear combination of products of LO Wilson coefficients weighted with colour factors. We include here only the contribution of the tree level operators Q_1 and Q_2, the penguin operators will be treated as a QCD correction and discussed below. Thus our result agrees, up to the phase space function, with the result for the decay $b \to c\bar{u}d$, see e.g. [72]:

$$\mathcal{N}_a = 3 C_1^{(0)2} + 3 C_2^{(0)2} + 2 C_1^{(0)} C_2^{(0)} . \quad (12)$$

The function g is the tree-level-phase-space-integral depending on the final-state-masses. Neglecting the strange quark mass, g reads (see e.g. Eq.(4.2) of [72] or [79] for an early reference):

$$\begin{aligned} g = & \sqrt{1-4x_c^2}\,(1-14x_c^2-2x_c^4-12x_c^6) \\ & +24x_c^4\,(1-x_c^4)\ln\left(\frac{1+\sqrt{1-4x_c^2}}{1-\sqrt{1-4x_c^2}}\right), \end{aligned} \tag{13}$$

where $x_c = m_c/m_b$ is the ratio of the charm- and the bottom-quark mass. The NLO correction can be split up into several contributions:

$$\Gamma^{(1)}_{c\bar{c}s} = \Gamma^{\alpha_s}_{c\bar{c}s} + \overline{\Gamma}^{m}_{c\bar{c}s} + \Gamma^{\rm PO}_{c\bar{c}s} + \Gamma^{C}_{c\bar{c}s} + \Gamma^{\rm PI}_{c\bar{c}s} + \Gamma^{Q_8}_{c\bar{c}s}. \tag{14}$$

The different terms of Eq.(14) are sorted according to their size. $\Gamma^{\alpha_s}_{c\bar{c}s}$ denotes corrections from the one gluon exchange in the LO diagrams within the effective theory. $\overline{\Gamma}^{m}_{c\bar{c}s}$ describes corrections of order $\mathcal{O}(\alpha_s)$ stemming from the translation of the b-quark mass from the pole- into the $\overline{\rm MS}$-scheme [80]. This term vanishes by definition if the pole-scheme is used for the b-quark mass. $\Gamma^{\rm PO}_{c\bar{c}s}$ contains LO contributions from the penguin operators $Q_{3\ldots6}$, which are treated as $\mathcal{O}(\alpha_s)$-effects in this paper. $\Gamma^{C}_{c\bar{c}s}$ describes NLO corrections to the Wilson-coefficients $C_{1,2}$. Besides these contributions, which were already calculated in [73] we also determined two previously neglected corrections: $\Gamma^{\rm PI}_{c\bar{c}s}$ and $\Gamma^{Q_8}_{c\bar{c}s}$ stem from insertions of the operators $Q_{1,2}$ and the operator Q_8 in penguin diagrams within the effective theory.
Below all these contributions will be discussed in detail.

2.3. Gluon-corrections to the insertion of $Q_{1,2}$ into treelevel diagrams

The largest $\mathcal{O}(\alpha_s)$-contribution stems directly from the next-to-leading term in Eq.(8). It arises from one-gluon corrections to the insertion of the operators Q_1 and Q_2 in tree-level diagrams of the effective theory, see Fig.(4). Hence, this term can be written as:

$$\Gamma^{\alpha_s}_{c\bar{c}s} = 8\Gamma_0|\xi_c|^2\cdot\left(C_2^{(0)2}g_{22} + C_1^{(0)2}g_{11} + \tfrac{2}{3}C_1^{(0)}C_2^{(0)}g_{12}\right). \tag{15}$$

Since we strictly expand in α_s and discard terms of $\mathcal{O}(\alpha_s^2)$, we use in Eq.(15) the LO expressions for the Wilson coefficients, denoted by $C_1^{(0)}$ and $C_2^{(0)}$. The functions g_{11}, g_{12} and g_{22} are given by phase-space-integrals over the corresponding diagrams, where one gluon is exchanged. For massless quarks

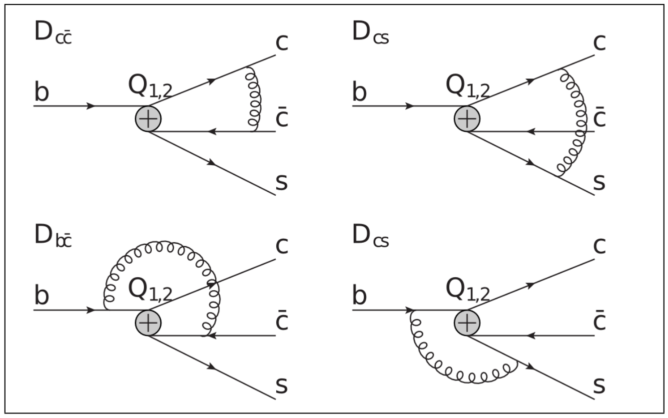

Figure 1: Virtual gluon corrections to the insertion of the operators Q_1 and Q_2 in tree-level diagrams of the effective theory. Only the diagrams that could not be taken from [83] and had to be be calculated anew, are shown. The corresponding diagrams with real gluon-emission are also not pictured.

these corrections were already calculated in 1981 by Altarelli et al. [81] and later confirmed in [82],

$$g_{11} = \frac{31}{4} - \pi^2 = g_{22} \, , \tag{16}$$

$$g_{12} = -\frac{7}{4} - \pi^2 \, . \tag{17}$$

For massive quarks the calculation is much more complicated and it was performed for the first time in 1995 [73]. However, most of the required corrections can be inferred from the work [83] by *Hokim* an *Pham*. There the exact width for a weak decay into three particles with arbitrary masses has been calculated up to order $\mathcal{O}(\alpha_s)$ in the full standard model, ignoring, however, the momentum-square in the $W^{\pm}$-propagator (as in the effective theory). Thus their result corresponds to the double insertion of the operator Q_2 into the next-to-leading term in Eq.(8). Using the notation of [83] the factor g_{22} can be expressed as

$$g_{22} = \frac{4}{\Omega_0} \left(\Gamma_l + \Gamma_u \right) . \tag{18}$$

The contributions on the right hand side of Eq.(18) are given in the formulæ (3.9), (3.36) and (4.34) of [83]. The arguments of theses functions have to be chosen as:

$$\rho_1 = \left(\frac{m_c}{m_b}\right)^2, \ \rho_2 = 0, \ \rho_3 = \left(\frac{m_c}{m_b}\right)^2. \tag{19}$$

Further information about using the results from [83] for the calculation of $\Gamma_{c\bar{c}s}$ is given in Appendix A.
Also the contributions from double insertions of the operator Q_1 can be inferred from [83], if the diagrams are Fierz-transformed. To do so, it was crucial to choose the evanescent operators in such a way that Fierz-symmetry is maintained at the one-loop-level. Following [84] we use:

$$E = \gamma_\mu \gamma_\nu \Gamma_\sigma \otimes \gamma^\sigma \gamma^\nu \Gamma^\mu - (4 - 8\varepsilon)\, \Gamma_\mu \otimes \Gamma^\mu, \tag{20}$$

where ε is the usual regulator in dimensional regularisation in $D = 4 - 2\varepsilon$ dimensions. Then we get for g_{11}:

$$g_{11} = \frac{4}{\Omega_0} \left(\Gamma'_l + \Gamma'_u\right), \tag{21}$$

The contributions on the right hand side of Eq.(21) are also given in the formulæ (3.9), (3.36) and (4.34) of [83], but now the arguments differ from (19), which is denoted by the apostrophe. They read instead:

$$\rho'_1 = 0, \ \rho'_2 = \left(\frac{m_c}{m_b}\right)^2, \ \rho'_3 = \left(\frac{m_c}{m_b}\right)^2. \tag{22}$$

Note, that in [83] diagrams containing a gluon exchange between the two different fermion-lines (i.e. the $b \to c$-line and the $\bar{c} \to s$-line) vanished due to the colour factor . As already mentioned, the results in [83] directly correspond to a double insertion of the operator Q_2 and they can also be used for the double insertion of the operator Q_1. However, in our calculation also a mixed contribution, i.e. an insertion of Q_1 and Q_2, arises, where the colour structure does not vanish, if a gluon is exchanged between the two different fermion-lines. The part of the contributions to g_{12}, where the gluon does not connect the two fermion lines can be extracted again from [83]. Four diagrams, where the gluon couples to both of the appearing fermion-lines, have to be computed new. These are the diagrams pictured in Figure 4. The four new contributions are denoted by $g_{c\bar{c}}$, g_{cs}, $g_{b\bar{c}}$ and g_{bs} and they are explicitly given in the Appendix B. Hence, we get for the last contribution in Eq.(15)

$$g_{12} = g_{22} + g_{c\bar{c}} + g_{cs} + g_{b\bar{c}} + g_{bs}. \tag{23}$$

These contributions have been calculated for the decay $b \to c\bar{u}d$ in [72]. Here one particle in the final state had to be taken massive. The decay $b \to c\bar{c}s$ was investigated in [73], where all particles in the final state are massive. Unfortunately the results in [73] contain several misprints and cannot be used for a numerical reanalysis, so they had to be calculated anew.

2.4. The $b-$quark mass in the $\overline{\mathrm{MS}}$*-scheme*

Since the pole mass suffers from renormalon ambiguities, as discussed e.g. in [85, 86], it has been argued, that the pole mass scheme is not well suited for performing precise calculations of inclusive decay rates, while short distance masses like the $\overline{\mathrm{MS}}$-mass [80] are better suited for this purpose [86]. The relation between the pole mass scheme and the $\overline{\mathrm{MS}}$-mass scheme is given as a power series in the strong coupling. Up to the order $\mathcal{O}(\alpha_s)$ it reads

$$m_q^{\mathrm{pole}} = \overline{m}_q(\mu_m)\left(1 + \frac{\alpha_s(\mu_m)}{\pi}\cdot\left[\frac{4}{3} - \ln\left(\frac{\overline{m}_q(\mu_m)^2}{\mu_m^2}\right)\right]\right). \qquad (24)$$

Therefore the translation between the two schemes creates additional $\mathcal{O}(\alpha_s)$-corrections in the total inclusive decay rates. These terms can be written as:

$$\overline{\Gamma}^{m}_{c\bar{c}s} = \Gamma^{(0)}_{c\bar{c}s}\left[\frac{80}{3} - 20\ln\left(\frac{m_b^2}{\mu_m^2}\right) - 8x_c\ln(x_c)\frac{d\ln(g)}{dx_c}\right], \qquad (25)$$

where g is the phase space function from Eq.(13). In LO there is a strong dependence on the scale μ_m, that appears in Eq.(24). The relation between the two mass schemes is, however, known very precisely - corrections up to order $\mathcal{O}(\alpha_s^3)$ have been calculated in [87], resulting in a small remaining scale dependence. Hence we consider the large LO scale dependence in Eq.(24) to be artificial and we do not vary that scale for our final numerics, but we set $\mu_m = m_b$ during the calculation. Thus the large logarithm in Eq. (25) vanishes.

Besides these two mass-schemes, we have also investigated three other quark mass schemes, the kinetic [88], the potential-subtracted (PS) [89] and the $\Upsilon(1S)$-scheme [90] for our calculation, see Section 3.4.

2.5. Contributions from the penguin-operators $Q_{3\ldots6}$

Besides the already discussed tree level diagrams, the decays $b \to c\bar{c}s$ can also occur via penguin diagrams. Therefore further contributions to the

$b \to c\bar{c}s$ width arise from the insertion of QCD penguin-operators $Q_{3...6}$ into tree diagrams of the effective theory. They can be written as:

$$\Gamma^{\rm PO}_{c\bar{c}s} = \frac{4\pi}{\alpha_s}\Gamma_0\left[\left(\Re\left(\xi_c\xi_t^*\right)\mathcal{N}_b + |\xi_t|^2\mathcal{N}_c\right)g + \left(\Re\left(\xi_c\xi_t^*\right)\mathcal{N}_d + |\xi_t|^2\mathcal{N}_e\right)g_+\right]. \quad (26)$$

Since this contribution is numerically of the order of the α_s-corrections, we decided to treat it formally as a QCD correction. But as no explicit factor $\alpha_s/4\pi$ appears in the calculation we need the factor $4\pi/\alpha_s$ in Eq.(26) to cancel the corresponding artificial factor in Eq.(14). The terms $\mathcal{N}_{b...e}$ are again combinations of Wilson coefficients and colour factors

$$\begin{aligned}
\mathcal{N}_b &= -2\Big(3C_1C_3 + C_1C_4 + 3C_2C_4 + C_2C_3\Big), &(27)\\
\mathcal{N}_c &= 3C_3^2 + 3C_4^2 + 2C_3C_4 + 3C_5^2 + 3C_6^2 + 2C_5C_6, &(28)\\
\mathcal{N}_d &= -2\Big(3C_1C_5 + C_1C_6 + 3C_2C_6 + C_2C_5\Big), &(29)\\
\mathcal{N}_e &= 2\Big(3C_3C_5 + C_3C_6 + 3C_4C_6 + C_4C_5\Big). &(30)
\end{aligned}$$

Here formally terms of order $\mathcal{O}\left(\alpha_s^2\right)$ appear, stemming from expressions of the form $C_i \cdot C_j$. These higher order terms have been discarded in the calculation to ensure a strict expansion up to order $\mathcal{O}\left(\alpha_s\right)$. They were only kept in Eq.(27-30) to enable a more compact notation. The appearing Wilson-coefficients $C_{3...6}$, as well as the coefficient $C_8^{(0)}$ appearing in Section 2.8, can be taken from [78].
The function g is the usual phase space factor, appearing first in Eq.(13), while g_+ is a different phase space integral, that appears when, an odd number of the factor $(1+\gamma_5)$ appears in the Dirac-structure. Its analytic expression, which was to our knowledge not shown before, reads:

$$\begin{aligned}
g_+ = 4x_c^2\Bigg[&\sqrt{1-4x_c^2}\,(1+5x_c^2-6x_c^4) &(31)\\
&+12x_c^2\,(1-2x_c^2+2x_c^4)\ln\left(\frac{2x_c}{1+\sqrt{1-4x_c^2}}\right)\Bigg].
\end{aligned}$$

Numerically g_+ agrees with Eq.(12) of [63]. Finally in Eq.(26) no approximation in the CKM-structure was used, as it is often done in the literature to eliminate ξ_t:

$$\xi_t = -\xi_c - \xi_u \approx -\xi_c. \quad (32)$$

Using this approximation our results in Eqs.(27-30) agree with the ones in the erratum of [63] and Eq.(27) and Eq.(29) agree with Eq.(XVII.14) from [78].

2.6. Order $\mathcal{O}(\alpha_s)$ corrections to the Wilson coefficients $C_{1,2}$

Since the Wilson coefficients C_1 and C_2 are given as a series in the strong coupling, see Eq.(5), they give rise to additional corrections of the order $\mathcal{O}(\alpha_s)$. These corrections are given by:

$$\Gamma^{C}_{c\bar{c}s} = \Gamma_0 |\xi_c|^2 g \Big[\Big(\frac{\alpha_s(M_W)}{\alpha_s(\mu)} - 1 \Big) \cdot \Big(4C_+^{(0)2} R_+ + 2C_-^{(0)2} R_- \Big) + \Big(4C_+^{(0)2} B_+ + 2C_-^{(0)2} B_- \Big) \Big]. \tag{33}$$

These contributions arise in all NLO QCD corrections to non-leptonic inclusive decays that are triggered via tree-level diagrams (with appropriate phase space functions), e.g. $b \to c\bar{u}d$ [72] and $b \to c\bar{c}s$ [73]. To simplify the notation we use here linear combinations of the operators Q_1 and Q_2, that do not mix under renormalisation, see e.g. [84]. This leads to the coefficients C_+ and C_-, which are defined as:

$$C_\pm = C_2 \pm C_1. \tag{34}$$

These coefficients can be written as (see e.g. [63])

$$C_\pm = C_\pm^{(0)} \left(1 + \frac{\alpha_s(M_W) - \alpha_s(\mu)}{4\pi} R_\pm + \frac{\alpha_s(\mu)}{4\pi} B_\pm \right), \tag{35}$$

with the leading order Wilson coefficients $C_\pm^{(0)}$, given by:

$$C_\pm^{(0)} = \left(\frac{\alpha_s(M_W)}{\alpha_s(\mu)} \right)^{\gamma_\pm^{(0)}/(2\beta_0)}. \tag{36}$$

β_0 is the leading coefficient of the QCD beta-function and $\gamma_\pm^{(0)}$ is the leading term of the anomalous dimensions of the operators Q_+ and Q_-. The coefficients read:

$$\beta_0 = 11 - \frac{2}{3} n_f = \frac{23}{3}, \tag{37}$$

$$\gamma_+^{(0)} = 4, \ \gamma_-^{(0)} = -8, \tag{38}$$

$$R_+ = \frac{10863 - 1278 n_f + 80 n_f^2}{6(33 - 2n_f)^2} = \frac{6473}{3174}, \tag{39}$$

$$R_- = -\frac{15021 - 1530 n_f + 80 n_f^2}{3(33 - 2n_f)^2} = -\frac{9371}{1587}, \tag{40}$$

$$B_\pm = \pm B \frac{N_C \mp 1}{2N_C}, \tag{41}$$

where $n_f = 5$ is the number of active quark flavours and $N_C = 3$ is the number of colours. The coefficient B from Eq.(41) is the only scheme dependent quantity in Eq.(33). In the NDR-scheme with the choice of evanescent operators as in Eq.(20) the scheme dependent factor B reads $B^{\text{NDR}} = 11$.

2.7. Insertions of $Q_{1,2}$ into penguin diagrams

Besides the corrections, in which the tree level diagrams are simply dressed with additional gluon lines (as discussed in Section 2.3), new contributions arise at order $\mathcal{O}(\alpha_s)$ due to insertions of the operators $Q_{1,2}$ into penguin diagrams, see Fig. 2. In principle both up and charm quarks could run in

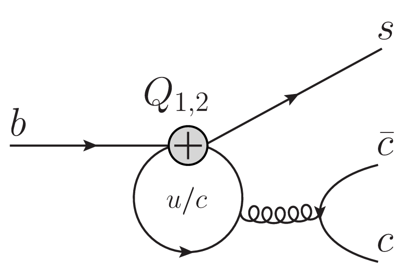

Figure 2: Insertion of the operators Q_1 and Q_2 into a penguin diagram of the effective theory. Compared to the penguin operators Q_3 - Q_6 these contributions appear with the large Wilson coefficient C_2.

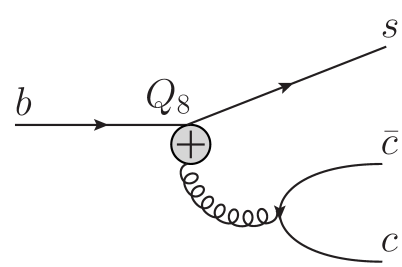

Figure 3: Insertion of the chromomagnetic operator Q_8 into a tree diagram of the effective theory.

the penguin loop, but because of the strong CKM-suppression, only the case with a charm quark is considered here. Insertions of this kind vanish for Q_1, since they involve a vanishing trace of a generator of the colour SU(3), so only Q_2 has to be considered.

The total contribution due to the insertion in penguin diagrams can then be written as:

$$\Gamma_{c\bar{c}s}^{\mathrm{PI}} = \frac{16}{3}\Gamma_0|\xi_c|^2\Re\left[C_2^{(0)2}\left(g_{\mathrm{PI}}+g_{\mathrm{PI}+}\right)\right], \tag{42}$$

where the functions g_{PI} and $g_{\mathrm{PI}+}$ are two phase-space-functions, which were calculated analytically for the first time. The exact expressions are given in Appendix C.

This corrections have until now only been included in the calculation of charm-less inclusive decay rates in [74], where they can be the dominant effect. Since the insertions into penguin diagrams are also expected to give sizable contributions to the b-quark decay into two charm quarks, we present them here for the first time. In our calculation the same loop integrals arise as in [74], but the phase space integration has to be performed for massive final state particles, while in [74] only massless final states were investigated. The insertion of the operator Q_2 in a penguin diagram can be decomposed in the following way:

$$Q_P = \sum_{i=3}^{6} r_i\left(s_{c\bar{c}}\right)Q_i. \tag{43}$$

Q_P denotes the operator generated by the penguin insertion and $r_i\left(s_{c\bar{c}}\right)$ are the appearing loop-functions which depend on the centre of mass energy $s_{c\bar{c}}$ of the c-$\bar{c}$-system. For the different r_i the following relation holds:

$$r_4 = r_6 = -3r_3 = -3r_5. \tag{44}$$

The function r_4 was calculated in [74] as

$$\begin{aligned} r_4 = \frac{1}{9s_{c\bar{c}}^{3/2}}\Bigg[& -3\sqrt{s_{c\bar{c}}-4m_c^2}\left(2m_c^2+s_{c\bar{c}}\right)\ln\left(\frac{\sqrt{1-4\frac{m_c^2}{s_{c\bar{c}}}}-1}{\sqrt{1-4\frac{m_c^2}{s_{c\bar{c}}}}+1}\right) \\ & +\sqrt{s_{c\bar{c}}}\left(-2\left(6m_c^2+s_{c\bar{c}}\right)+3s_{c\bar{c}}\ln\left(\frac{m_c^2}{\mu^2}\right)\right)\Bigg]. \end{aligned} \tag{45}$$

As in the case of the LO contributions discussed in Section 2.5 two different functions appear for the insertions into penguin diagrams, depending on whether the number of vertices that involve the factor $(1+\gamma_5)$ is even (g_{PI}) or odd ($g_{\mathrm{PI}+}$).

2.8. Contributions from the chromomagnetic operator Q_8

Additional order $\mathcal{O}(\alpha_s)$ contributions arise through insertions of the chromomagnetic operator Q_8, see Figure 3. After a straight-forward calculation, these contributions can be written as:

$$\Gamma_{c\bar{c}s}^{Q_8} = 3\Gamma_0 C_8^{(0)} g_{Q8} \left[\Re\left(\xi_t \xi_c^*\right) C_2^{(0)} - |\xi_t|^2 \left(C_4^{(0)} + C_6^{(0)} \right) \right]. \tag{46}$$

The phase space factor g_{Q8}, which was calculated here for the first time, is given as:

$$g_{Q8} = 32 \left[\frac{1 - 20x_c^2 + 52x_c^4 + 48x_c^6}{9\sqrt{1-4x_c^2}} + \frac{8}{3} x_c^4 \left(2x_c^2 - 3\right) \ln\left(\frac{2x_c}{1+\sqrt{1-4x_c^2}} \right) \right]. \tag{47}$$

3. Investigation of the NLO-result for $\Gamma_{c\bar{c}s}$

With all the contributions, which were calculated in Section 2, the total decay width of the inclusive decay $b \to c\bar{c}s$ can be written in NLO-QCD as:

$$\Gamma_{c\bar{c}s} = \Gamma_{c\bar{c}s}^{(0)} + \frac{\alpha_s}{4\pi} \left(\Gamma_{c\bar{c}s}^{\alpha_s} + \overline{\Gamma}_{c\bar{c}s}^{m} + \Gamma_{c\bar{c}s}^{\mathrm{PO}} + \Gamma_{c\bar{c}s}^{C} + \Gamma_{c\bar{c}s}^{\mathrm{PI}} + \Gamma_{c\bar{c}s}^{Q_8} \right). \tag{48}$$

In the following chapter, the obtained results will be investigated in detail. First we provide some consistency checks, next we perform a numerical analysis of the inclusive decay rate and we also discuss several conceptual issues, like different definitions of quark masses.

3.1. Scheme-independence

Here we show the independence of our results on the renormalisation scheme used for γ_5. The calculation of the correction g_{12} in Section 2.3 involved UV-divergences and the result depends on the treatment of γ_5 in dimensional regularisation. The only source of these divergences is the loop integral $\mathtt{C}_{00}$ in the notation of *LoopTools* [91]. Thus, the scheme dependence of the overall result is completely encoded in the terms:

$$\mathtt{C}_{00} + B_1, \tag{49}$$

for $g_{c\bar{c}}$ and g_{bs} and

$$\mathtt{C}_{00} + B_2, \tag{50}$$

for g_{cs} and $g_{b\bar{c}}$. The terms B_1 and B_2 contain all the scheme-dependence. Since they are just numbers, the phase space integration can be performed analytically, and one obtains for the total scheme dependent part:

$$\Gamma_{c\bar{c}s}^{\alpha_s \text{scheme}} = \frac{16}{3}\Gamma_0 |\xi_c|^2 g \left(8B_1 - 32B_2\right) C_1^{(0)} C_2^{(0)}. \tag{51}$$

This scheme dependence has to be cancelled by the scheme dependence of the Wilson coefficients $C_{1,2}$, which can be obtained from (33) to be:

$$\Gamma_{c\bar{c}s}^{C \text{scheme}} = \frac{16}{3}\Gamma_0 |\xi_c|^2 g B C_1^{(0)} C_2^{(0)}. \tag{52}$$

For the whole result to be scheme-independent, the following combination needs to have the same value in all schemes:

$$B + 8B_1 - 32B_2. \tag{53}$$

In the NDR and in the t'Hooft-Veltman-scheme one gets [84]

$$\begin{array}{llllllll} B^{\rm NDR} & = & 11, & B_1^{\rm NDR} & = & -\frac{1}{2}, & B_2^{\rm NDR} & = -\frac{1}{16}, \\ B^{\rm HV} & = & 7, & B_1^{\rm HV} & = & 0, & B_2^{\rm HV} & = -\frac{1}{16}. \end{array} \tag{54}$$

This shows the scheme independence of the final result.

3.2. Analytical comparison with the literature

Next we compare our results with the calculation of the decay rate $\Gamma_{c\bar{c}s}$ in [73], where the contributions calculated in Section 2.3 have been determined already in 1995. Using the formulae given in [73] we found, however, that the final result is IR divergent. Hence, we present here a careful comparison of the individual contributions.
We denote with D_{xy} the diagrams, where the gluon connects the x-quark with the y-quark. In [72] and [73] a different notation was used, the transcription reads:

$$\begin{array}{llll} \text{Diagram} & \textbf{VI} & \leftrightarrow & D_{c\bar{c}}\ , \\ \text{Diagram} & \textbf{VIII} & \leftrightarrow & D_{cs}\ , \\ \text{Diagram} & \textbf{X} & \leftrightarrow & D_{b\bar{c}}\ , \\ \text{Diagram} & \textbf{XI} & \leftrightarrow & D_{bs}\ . \end{array} \tag{55}$$

For the virtual corrections (i.e. the three-particle-cuts in the notation of [73]), the coefficients in front of the loop functions could be compared and we found, that the virtual results for the diagram $D_{c\bar{c}}$ coincide. For the diagrams D_{cs} and $D_{b\bar{c}}$ a factor -1 is missing in the results of [73]. In the diagram D_{bs} the difference is, however, a little more subtle. Eq.(20) in [73]

$$\mathrm{Im}\big[\mathrm{XI}+\mathrm{XI}^\dagger\big]^{(3)} = \frac{g^2}{192\pi^5 b}\int_{4c}^{b}\frac{\mathrm{d}t}{t}(b-t)^2 v\Big\{(t+2c)b\big[t(A+4B)+(t+2b)\tilde{B}\ldots, \tag{56}$$

has to be modified to

$$\mathrm{Im}\big[\mathrm{XI}+\mathrm{XI}^\dagger\big]^{(3)} = \frac{g^2}{192\pi^5 b}\int_{4c}^{b}\frac{\mathrm{d}t}{t}(b-t)^2 v\Big\{(t+2c)b\big[t(A-2B)+2(b-t)\tilde{B}\ldots . \tag{57}$$

These two expressions would be equal, if $2B+\tilde{B}=0$ holds, which is clearly not the case. For the real corrections (i.e. the four-particle-cuts in the notation of [73]) our results coincide with the ones in [73] for the diagrams $D_{c\bar{c}}$ and D_{cs}. For the two remaining diagrams, no agreement could be found. Since in [73] these contributions are given in terms of some phase space functions $\mathcal{K}_{0\ldots7}$, while the results obtained here are just single expressions, the error could not be traced back easily.

3.3. Numerical comparison with the literature

Using the input parameters from [73] for our newly calculated expressions for g_{11}, g_{12} and g_{22}, we could reproduce all numerical results quoted in Table 2 of [73], even though several analytic expressions in g_{12} differed, as discussed in detail in Section 3.2. Hence we conclude, that the results in [73] contain simply several misprints[4].

[4] Since the authors of [73] are not active in HEP anymore, we could not settle this issue without performing the calculation anew.

3.4. Numerical results for the decay width

For our up-to-date numerical evaluation we used the following input parameters from [1, 92]:

$$\begin{array}{lcll} \overline{m}_b\,(\overline{m}_b) & = & (4.25 \pm 0.05) & \text{GeV}\,, \\ \overline{m}_s\,(\overline{m}_b) & = & (0.085) & \text{GeV}\,, \\ \Lambda_{QCD} & = & (0.213 \pm 0.008) & \text{GeV}\,, \\ |V_{us}| & = & 0.225 \pm 0.001\,, & \\ |V_{ub}| & = & 0.004 \pm 0.001\,, & \\ |V_{cb}| & = & 0.041 \pm 0.001\,, & \\ \delta_{CKM} & = & 71^\circ \pm 25^\circ\,. & \end{array} \tag{58}$$

The remaining CKM elements were inferred from the unitarity of the CKM matrix. The decay rate $\Gamma(b \to c\bar{c}s)$ has a strong dependence on the charm quark mass, where a lot of progress has been made in its accurate determination in recent years. We use the following three values [5] for our numerics:

$$\begin{array}{lcll} a): \overline{m}_c\,(\overline{m}_c) & = & (1.273 \pm 0.006) & \text{GeV}\,, \\ b): \overline{m}_c\,(\overline{m}_c) & = & (1.279 \pm 0.013) & \text{GeV}\,, \\ c): \overline{m}_c\,(\overline{m}_c) & = & (1.277 \pm 0.026) & \text{GeV}\,. \end{array} \tag{59}$$

$a)$ stems from [94], $c)$ from [95] and $c)$ from [96]. The central values of these three determinations agree excellently, the error estimates range from 0.5% [94] to 2% [96], which has a visible effect in our numerical analysis. With these inputs, the following value for the total width is obtained:

$$\Gamma^{a)}_{c\bar{c}s} = \Gamma_0 |V_{cb}|^2 \left(1.64 \pm 0.15_\mu \pm 0.04_{m_b} \pm 0.02_{m_c} \pm 0.03_{\Lambda_{QCD}}\right), \tag{60}$$

$$\Gamma^{b)}_{c\bar{c}s} = \Gamma_0 |V_{cb}|^2 \left(1.62 \pm 0.15_\mu \pm 0.04_{m_b} \pm 0.05_{m_c} \pm 0.03_{\Lambda_{QCD}}\right), \tag{61}$$

$$\Gamma^{c)}_{c\bar{c}s} = \Gamma_0 |V_{cb}|^2 \left(1.63 \pm 0.15_\mu \pm 0.04_{m_b} \pm 0.10_{m_c} \pm 0.03_{\Lambda_{QCD}}\right). \tag{62}$$

All three determinations agree perfectly, the only sizable difference is in the theoretical error due to the charm quark mass, which ranges from 1% to 6%. Since the factor $\Gamma_0 |V_{cb}|^2$ cancels in most branching ratios exactly, we did not include this term in the error analysis. The individual contributions to the inclusive decay width are given in Table 1, where also all parametric uncertainties are listed. These results will be discussed below in detail.

[5] See also [93] for another recent determination.

		$\delta\mu$	δm_c	δm_b	$\delta\Lambda_{QCD}$
$\Gamma^{(0)}_{c\bar{c}s}$	1.37	± 0.11	± 0.07	± 0.04	± 0.02
$\Gamma^{\alpha_s}_{c\bar{c}s}$	0.34	± 0.07	± 0.01	± 0.00	± 0.01
$\overline{\Gamma}^{m}_{c\bar{c}s}$	0.12	± 0.03	± 0.03	± 0.01	± 0.01
$\Gamma^{\rm PO}_{c\bar{c}s}$	-0.09	± 0.04	± 0.00	± 0.00	± 0.00
$\Gamma^{C}_{c\bar{c}s}$	-0.07	± 0.04	± 0.00	± 0.00	± 0.00
$\Gamma^{\rm PI}_{c\bar{c}s}$	-0.05	± 0.01	± 0.00	± 0.00	± 0.00
$\Gamma^{Q_{\rm S}}_{c\bar{c}s}$	0.01	± 0.00	± 0.00	± 0.00	± 0.00
$\Gamma_{c\bar{c}s}$	1.63	± 0.15	± 0.10	± 0.04	± 0.03

Table 1: Single contributions to the $c\bar{c}s$-decay width in units of $\left(\Gamma_0|V_{cb}|^2\right)$ and the corresponding errors.

As the main numerical result of our paper we present new values for the branching ratio of the inclusive $b \to c\bar{c}s$ transition.

$$Br(b \to c\bar{c}s) \;\; = \;\; \frac{\Gamma_{c\bar{c}s}}{\Gamma_{tot}}\,. \tag{63}$$

For the total decay rate Γ_{tot} we took all theoretical expressions that were available in the literature, $b \to cl^-\bar{\nu}$ from [71], $b \to c\bar{u}d$ from [72], $b \to c\bar{c}s$ from this work, $b \to$ no charm from [74] and $b \to sg$ from [75, 76]. We finally get

$$Br(b \to c\bar{c}s)^{a)} \;\; = \;\; 0.234 \pm 0.002_\mu \pm 0.003_{m_b} \pm 0.001_{m_c} \pm 0.001_{\Lambda_{QCD}}\,, \tag{64}$$

$$Br(b \to c\bar{c}s)^{b)} \;\; = \;\; 0.232 \pm 0.002_\mu \pm 0.003_{m_b} \pm 0.003_{m_c} \pm 0.001_{\Lambda_{QCD}}\,, \tag{65}$$

$$Br(b \to c\bar{c}s)^{c)} \;\; = \;\; 0.232 \pm 0.002_\mu \pm 0.003_{m_b} \pm 0.006_{m_c} \pm 0.001_{\Lambda_{QCD}}\,. \tag{66}$$

The errors in the branching ratios are considerably smaller than in the decay rate, obviously several uncertainties cancel to some extend in the branching ratios. Our final results show several interesting features (to be conservative we will use in the following the value of [96] for the charm quark mass):

- All NLO-QCD corrections enhance the LO-QCD result for the decay rate by +19%. The contribution of the 1-loop gluon correction to the insertion of the operators Q_1 and Q_2 is even $+25\%$ of the LO-QCD result. As already pointed out in [70, 73], effects of a finite charm quark mass were crucial. This can be seen if one compares our results with the one for a vanishing charm quark mass:

$$\Gamma_{c\bar{c}s}^{(\overline{m}_c=0)} = \Gamma_0|V_{cb}|^2 \left(3.17^{(0)} - 0.07^{\alpha_s} + \overline{0.37}^{m} - 0.14^{\rm PO} - 0.16^{C} - 0.08^{\rm PI} + 0.03^{Q_8}\right) . \tag{67}$$

Because of the missing phase space suppression the LO contribution is now more than a factor 2 larger than in Table 1. The biggest dependence is found, however, in $\Gamma_{c\bar{c}s}^{\alpha_s}$, which changes from $-0.07\ \Gamma_0|V_{cb}|^2$ in the massless case to $+0.34\ \Gamma_0|V_{cb}|^2$ in the massive case.

- All penguin effects give a contribution of about -9% of the LO-QCD decay rate. The newly calculated penguin insertions are of a similar size as some of the theoretical uncertainties, so their inclusion is reasonable. Gluon corrections to the insertion of the penguin operators $Q_3, ..., Q_6$ in tree level diagrams of the effective theory are still missing. Naively one expects these corrections to be of the order of

$$\frac{\Gamma_{c\bar{c}s}^{\alpha_s}}{\Gamma_{c\bar{c}s}^{(0)}} \Gamma_{c\bar{c}s}^{PO} \approx \frac{0.34}{1.37}\, 0.09 \approx 0.02\ .$$

  This is much smaller than the parametric uncertainties of our results. Hence, we consider the effort of the corresponding NLO-QCD calculation not to be justified.

- The dominant theoretical uncertainty in our above analysis stems from the renormalisation scale dependence. It is of the order of $\pm 9\%$ of the decay rate and cancels in the branching ratio to a remaining uncertainty of the order of $\pm 1\%$. To reduce this uncertainty further a NNLO-QCD calculation would be mandatory. The dependence on the values of the charm quark mass and the bottom quark mass is already subleading, as well as the dependence on the strong coupling.
  The dominant dependence of the decay rate on the CKM elements is given by the overall factor $|V_{cb}|^2$, which results in an uncertainty of about 5%. Since we are interested in the end in experimentally measurable branching ratios we did not include the prefactor $\Gamma_0|V_{cb}|^2$, which cancels exactly in the ratios, in the error analysis of the decay rate. The remaining CKM dependence is negligible.

We also investigated the effect of a non-vanishing strange quark mass and got for $\overline{m}_s\,(\overline{m}_b) = 0.085\,\mathrm{GeV}$

$$\Gamma_{c\bar{c}s} = \Gamma_0 |V_{cb}|^2 \left(1.62 \pm 0.15_\mu \pm 0.04_{m_b} \pm 0.10_{m_c} \pm 0.03_{\Lambda_{QCD}}\right) \,, \quad (68)$$

which is almost equivalent to Eq.(62). So this effect can be safely neglected.

- In [41] it was shown that using $\overline{m}_c(\overline{m}_b)$ instead of $\overline{m}_c(\overline{m}_c)$ sums up large logarithms of the form $x_c^2 \ln x_c^2$ to all orders. We use this prescription also in this work, which also solves a second issue: one might consider the natural scale of the decay $b \to c\bar{c}s$ to be $\sqrt{m_b^2 - 4m_c^2}$. Using our numerical input we get for the renormalisation scale $\mu = \sqrt{1 - 4(\overline{m}_c(\overline{m}_b) m_c / \overline{m}_b(\overline{m}_b))^2}\; m_b \approx 0.9\; m_b$, which is very close to our choice $\mu = m_b$. Thus we see no reason for choosing different renormalisation scales in different b-decay channels. Choosing different scales would enhance the theoretical uncertainties in the branching ratios sizable.

- Since we are claiming a high precision of our final result, hypothetical drawbacks of our theoretical tools have to be investigated in detail. For the calculation of inclusive decay rates within the HQE, one has to take in to account **all** possible cuts through the corresponding forward-scattering diagrams. In the case of penguin insertions and contributions from Q_8, some cuts, however, do not belong to $b \to c\bar{c}s$, but to the decay $b \to sg$, see Fig.(4). Such a feature could in principle spoil

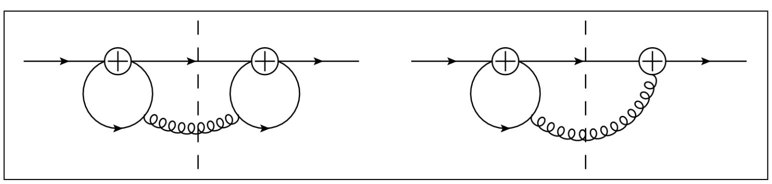

Figure 4: Cuts through forward scattering diagrams related to penguin insertions and Q_8-contributions, which belong not to $b \to c\bar{c}s$ but to the $b \to sg$ decay.

the application of the HQE to the decay $b \to c\bar{c}s$. All these cuts however involve a quark-loop from which a real gluon is emitted. The corresponding matrix element can be expressed as:

$$\begin{aligned} \mathcal{M} \propto & \left(m_l^2 B_0 + (2-D)\, B_{00}\right) \bar{s} \not{\epsilon}^* \,(1-\gamma_5)\, b \\ & + (B_1 + B_{11})\,(2-D)\, \bar{s} \not{p}_g \not{\epsilon}^* \not{p}_g \,(1-\gamma_5)\, b, \end{aligned} \quad (69)$$

where the B_{ij} are the two-point loop-integrals and p_g^μ and ϵ^μ are the gluon's momentum- and polarisation vector. m_l is the mass of the particle running in the loop. The second line of (69) vanishes due to the on-shell condition of the gluon: $p_g^\mu p_{g\mu} = p_g^\mu \epsilon_\mu^* = 0$.
For a vanishing momentum-square of the gluon, the remaining loop-functions, B_0 and B_{00}, are related by:

$$B_{00} = \frac{m_l^2}{2} \frac{1}{1-\varepsilon} B_0, \tag{70}$$

in $D = 4 - 2\varepsilon$ dimensions. With this relation, also the first line of (69) vanishes and these dangerous cuts do not contribute.

- Finally we compare the numerical values for the branching ratio of $b \to c\bar{c}s$ for different schemes of the b-quark mass. We use the pole scheme, the $\overline{MS}$-scheme [80], the kinetic [88], the potential-subtracted (PS) [89] and the $\Upsilon(1s)$-scheme [90]. Our final results in these schemes reads:

$$\begin{aligned} \mathcal{B}_{c\bar{c}s}^{\text{Pole}} &= 0.166 \pm 0.011 \,, && (71) \\ \mathcal{B}_{c\bar{c}s}^{\overline{\text{MS}}} &= 0.232 \pm 0.007 \,, && (72) \\ \mathcal{B}_{c\bar{c}s}^{\Upsilon} &= 0.243 \pm 0.013 \,, && (73) \\ \mathcal{B}_{c\bar{c}s}^{\text{PS}} &= 0.241 \pm 0.013 \,, && (74) \\ \mathcal{B}_{c\bar{c}s}^{\text{KIN}} &= 0.245 \pm 0.013 \,. && (75) \end{aligned}$$

  Except for the pole mass scheme all other quark mass schemes agree very nicely, the largest shift is found in the kinetic scheme, which is about 0.013, i.e. 6% larger than the result in the MS scheme. Since the pole scheme has theoretical disadvantages, as discussed in Section 2.4, we will not use the result in this scheme. The numerical difference in the remaining four schemes will be used as an estimate for an additional systematic uncertainty, which we estimate to be ± 0.013.

Thus we get as our final result for the branching ratio

$$\mathcal{B}_{c\bar{c}s} = 0.232 \pm 0.007 \pm 0.013 \approx (23 \pm 2)\% \,. \tag{76}$$

4. Conclusion

In this work, the width for the inclusive decay channel $b \to c\bar{c}s$ was computed up to the order $\mathcal{O}(\alpha_s)$ within the framework of the HQE. This theoretical framework passed recently a non-trivial experimental test: the measured value of the decay rate difference $\Delta\Gamma_s$ in the neutral B_s meson system agrees nicely with the corresponding standard model prediction [44]. Another very non-trivial test is related to the huge lifetime difference in the D-meson systems. Here first results, although suffering from huge hadronic uncertainties, look very promising [45]. Thus an updated prediction of $\Gamma(b \to c\bar{c}s)$ within the framework of the HQE is clearly overdue.
For that purpose we had to recalculate radiative corrections to insertions of the dominant operators Q_1 and Q_2 in tree level diagrams of the effective theory. This task was already performed in [73], but the formulæ in [73] contain several misprints. We give the corrected expressions in the appendix of this paper. However, numerical results of [73] could be exactly reproduced. In addition to that we also determined for the first time NLO-QCD contributions from insertions of the operators Q_1 and Q_2 in penguin diagrams of the effective theory, as well as contributions from the chromomagnetic operator Q_8.
Combining our new calculation with the impressive improvements in the accurate determination of standard model parameters like quark masses and CKM parameters we obtain as the main numerical result a very precise value of the branching ratio of the decay $b \to c\bar{c}s$

$$Br(b \to c\bar{c}s) = (23 \pm 2)\% \, . \tag{77}$$

Further support for this small error is given by new insights in different quark mass schemes.
With this new result a re-analysis of the semileptonic branching-ratio $\mathcal{B}_{Sl}$ and the charm-multiplicity n_c can be performed, see [97]. Such an analysis will lead to important and complementary insights on the possible size of new physics effects in B decays.

Acknowledgments

We would like to thank M. Gorbahn, A. Kagan, G. Kirilin, U. Nierste and J. Rohrwild for enlightening discussions; C. Davies, A. Hoang and M. Steinhauser for helpful comments and also E. Bagan and B. Fiol for trying to dig out their old computer programs. F.K. and T.R. would like to thank the IPPP Durham and KIT Karlsruhe for hospitality. In addition, F.K. and T.R. would like to thank M. Beneke and A. Ibarra for support during their thesis.

Appendix A. An introduction to [83]

The corrections to the tree level-diagrams, that involve gluons coupling to only one fermion-line were given in the paper [83] in terms of a one dimensional integral. For example the term g_{22} can be expressed as:

$$g_{22} = \frac{4}{\Omega_0} \left(\Gamma_l + \Gamma_u \right) . \tag{A.1}$$

Here, as in this whole section, the notation of [83] is used. The two contributions Γ_l and Γ_u depend on the mass ratios $\rho_i = (m_i/M)^2$. Γ_u hereby contains all effects due to gluon-exchanges on the upper vertex, the vertex with the decaying particle incoming and one particle outgoing. In the $b \to c\bar{c}s$-case, the upper vertex is the b-c-W^--vertex. Γ_l contains the corrections from gluon exchanges on the lower vertex, which in this case is the $\bar{c}$-s-W^--vertex. As already mentioned, diagrams that contain gluon-exchanges between upper and lower vertex vanish due to the colour-structure. The factor Ω_0 is given by equation (3.9) in [83].
As usual for such radiative corrections, the $\Gamma_{u,l}$ each consist of a part describing virtual- and real-gluon-effects respectively:

$$\begin{aligned} \Gamma_u &= \Gamma_l^v + \Gamma_l^b, && \text{(A.2)} \\ \Gamma_l &= \Gamma_u^v + \Gamma_u^b, && \text{(A.3)} \end{aligned}$$

which are defined in equations (3.36) and (4.34) as one dimensional integrals over the functions $R_{l,u}^{b,v}(\xi)$ respectively. These are given in equations (3.11), (3.35), (4.7) and (4.33).

Appendix B. Expressions for the radiative corrections

The expressions for the $\mathcal{O}(\alpha_s)$ corrections to $b \to c\bar{c}s$ are split in a virtual part, e.g. $g_{c\bar{c}}^{\mathrm{v}}$, stemming from loop-corrections, and a real part $g_{c\bar{c}}^{\mathrm{r}}$ from gluon radiation. The sums of both contributions, $g_x = g_x^{\mathrm{v}} + g_x^{\mathrm{r}}$, are infrared-finite for every diagram, as expected.

Appendix B.1. Expressions for the virtual contributions

The virtual correction $g^{\rm v}_{c\bar{c}}$ reads with the infrared-regulator $\xi = m_g/m_b$:

$$g^{\rm v}_{c\bar{c}} = \int_{4x_c^2}^{1} dz_{12} \tfrac{-4}{z_{12}^{3/2}} \left(1-z_{12}\right)^2 \sqrt{z_{12}-4x_c^2} \Bigg[z_{12}\left(1+2z_{12}\right)\big[-2\left(\mathtt{C}_{00}+B_1\right) +\mathtt{C}_0 z_{12}+\mathtt{C}_1 z_{12}+\mathtt{C}_{12} z_{12}+\mathtt{C}_2 z_{12}\big] + 2x_c^4\big[-2\mathtt{C}_2+2\mathtt{C}_0\left(z_{12}-1\right) +2\mathtt{C}_1\left(z_{12}-1\right)+3\mathtt{C}_{11}z_{12}+9\mathtt{C}_{12}z_{12}+2\mathtt{C}_2 z_{12}\big] +x_c^2\Big[4\left(\mathtt{C}_{00}+B_1\right)\left(z_{12}-1\right)-\big[3\mathtt{C}_1+4\mathtt{C}_{12}+3\mathtt{C}_2\big]z_{12} -\big[6\mathtt{C}_0+9\mathtt{C}_1+3\mathtt{C}_{11}+11\mathtt{C}_{12}+9\mathtt{C}_2\big]z_{12}^2\Big]\Bigg]. \tag{B.1}$$

The functions $\mathtt{C_{ij}}$ are the three-point-functions as used in the *LoopTools*-package [91], their arguments read in the notation adapted in the *LoopTools*-manual: $p_1^2 = (p_1+p_2)^2 = m_2^2 = m_3^2 = x_c^2$, $p_2^2 = z_{12}$ and $m_1^2 = \xi^2$. The arguments are chosen in a way that renders the loop-functions dimensionless. Therefore, also the renomalization-point is set to μ^2/m_b^2.

The function $g^{\rm v}_{cs}$ is given by:

$$g^{\rm v}_{cs} = \int_{x_c^2}^{(1-x_c)^2} dz_{12} \tfrac{-12}{z_{12}} \left(z_{12}-x_c^2\right)^2\left(1+x_c^2-z_{12}\right) \sqrt{x_c^4+\left(1-z_{12}\right)^2-2x_c^2\left(1+z_{12}\right)}\Big[16\left(\mathtt{C}_{00}+B_2\right)+4\mathtt{C}_1x_c^2+4\mathtt{C}_{11}x_c^2 +4\mathtt{C}_{12}x_c^2+2\mathtt{C}_2x_c^2+2\mathtt{C}_0\left(x_c^2-z_{12}\right)-2\mathtt{C}_1z_{12}-4\mathtt{C}_{12}z_{12}-2\mathtt{C}_2z_{12}\Big]. \tag{B.2}$$

Here the arguments of the *LoopTools*-functions are given by: $p_1^2 = m_2^2 = x_c^2$, $(p_1+p_2)^2 = m_3^2 = 0$, $p_2^2 = z_{12}$ and $m_1^2 = \xi^2$.

The third virtual correction is given by:

$$g^{\rm v}_{b\bar{c}} = \int_{x_c^2}^{(1-x_c)^2} \tfrac{-12}{z_{12}} \left(z_{12}-x_c^2\right)^2 \sqrt{x_c^4+\left(1-z_{12}\right)^2-2x_c^2\left(1+z_{12}\right)} \Big[4\mathtt{C}_1+4\mathtt{C}_{11}+4\mathtt{C}_{12}+2\mathtt{C}_2+2\mathtt{C}_1x_c^2+4\mathtt{C}_{11}x_c^2+12\mathtt{C}_{12}x_c^2+2\mathtt{C}_2x_c^2+2\mathtt{C}_1x_c^4 +8\mathtt{C}_{12}x_c^4+4\mathtt{C}_2x_c^4+16\left(\mathtt{C}_{00}+B_2\right)\left(1+x_c^2-z_{12}\right)+2\mathtt{C}_0\left(1+x_c^2-z_{12}\right)^2 -6\mathtt{C}_1z_{12}-4\mathtt{C}_{11}z_{12}-8\mathtt{C}_{12}z_{12}-4\mathtt{C}_2z_{12}-4\mathtt{C}_1x_c^2z_{12}-12\mathtt{C}_{12}x_c^2z_{12} -6\mathtt{C}_2x_c^2z_{12}+2\mathtt{C}_1z_{12}^2+4\mathtt{C}_{12}z_{12}^2+2\mathtt{C}_2z_{12}^2\Big]. \tag{B.3}$$

The three-point-functions' arguments are: $p_1^2 = m_2^2 = 1$, $(p_1+p_2)^2 = m_3^2 = x_c^2$, $p_2^2 = z_{12}$ and $m_1^2 = \xi^2$.

The last virtual correction reads:

$$
\begin{aligned}
g_{bs}^{\mathrm{v}} = \textstyle\int_{4x_c^2}^{1} dz_{12} \tfrac{-4}{z_{12}^{3/2}} \left(1-z_{12}\right)^2 \sqrt{z_{12}-4x_c^2} \Big[-2x_c^2 \big[2\left(\mathtt{C}_{00}+B_1\right)+\mathtt{C}_1+\mathtt{C}_2 \\
+\mathtt{C}_0 \left(1-z_{12}\right)^2 - 2\left(\mathtt{C}_{00}+B_1\right) z_{12} - 2\mathtt{C}_1 z_{12} - 3\mathtt{C}_{11} z_{12} - \mathtt{C}_{12} z_{12} - 2\mathtt{C}_2 z_{12} \\
+\mathtt{C}_1 z_{12}^2 + \mathtt{C}_{12} z_{12}^2 + \mathtt{C}_2 z_{12}^2 \big] + z_{12} \big[-2\left(\mathtt{C}_{00}+B_1\right) - \mathtt{C}_1 - \mathtt{C}_2 - 4\left(\mathtt{C}_{00}+B_1\right) z_{12} \\
-4\mathtt{C}_1 z_{12} - 3\mathtt{C}_{11} z_{12} - 2\mathtt{C}_{12} z_{12} - \mathtt{C}_2 z_{12} + 2\mathtt{C}_1 z_{12}^2 + 2\mathtt{C}_{12} z_{12}^2 + 2\mathtt{C}_2 z_{12}^2 \\
+\mathtt{C}_0 \left(2z_{12}^2 - z_{12} - 1\right) \big] \Big].
\end{aligned}
\tag{B.4}
$$

The arguments of the loop-functions are: $p_1^2 = m_2^2 = 1$, $(p_1+p_2)^2 = m_3^2 = 0$, $p_2^2 = z_{12}$ and $m_1^2 = \xi^2$.
Like in section 3.1, the two coefficients $B_{1,2}$ encode the scheme-dependence of the results. They always appear in the combination $\mathtt{C}_{00}+B_{1,2}$, since $\mathtt{C}_{00}$ is the only UV-divergent integral. In the NDR- and HV-scheme, these coefficients are given by:

$$
B_1^{\mathrm{NDR}} = -\frac{1}{2},\ B_2^{\mathrm{NDR}} = -\frac{1}{16},\ B_1^{\mathrm{HV}} = 0,\ B_2^{\mathrm{HV}} = -\frac{1}{16}. \tag{B.5}
$$

Appendix B.2. Expressions for the real parts

The corresponding real corrections read, again with $\xi = m_g/m_b$ as an infrared regulator:

$$
\begin{aligned}
g^{\rm r}_{c\bar{c}} = & \int_{(2x_c+\xi)^2}^{1} dz_{123} \int_{(x_c+\xi)^2}^{(\sqrt{z_{123}}-x_c)^2} dz_{12}(-6)\,(z_{123}-1)^2 \Bigg[-(z_{12}-x_c^2) \\
& \Big[x_c^4+(z_{12}-z_{123})^2-2x_c^2\,(z_{12}+z_{123})\Big]^{5/2}\Big[-3x_c^4\,(2+z_{123})-z_{12}^2\,(2+z_{123}) \\
& +z_{12}z_{123}\,(2+z_{123})+2z_{123}^2\,(1+2z_{123})+x_c^2\big(-3z_{123}^2+4z_{12}\,(2+z_{123})\big)\Big] \\
& +2z_{12}\big(x_c^4+(z_{12}-z_{123})^2-2x_c^2\,(z_{12}+z_{123})\big)^2\Big[x_c^6\,(2+z_{123}) \\
& -(z_{12}-z_{123})\,z_{123}^2\,(1+2z_{123})-x_c^4\big[-3\,(z_{123}-1)\,z_{123}+2z_{12}\,(2+z_{123})\big] \\
& +x_c^2\big(z_{12}\,(z_{123}-1)\,z_{123}+z_{123}^2-4z_{123}^3+z_{12}^2\,(2+z_{123})\big)\Big] \\
& \Bigg[\ln\Bigg(-x_c^4+z_{12}\,(z_{12}-z_{123})-(z_{12}+z_{123})\,\xi^2+x_c^2\,(z_{123}+\xi^2)- \\
& \sqrt{x_c^4+(z_{12}-z_{123})^2-2x_c^2\,(z_{12}+z_{123})}\sqrt{x_c^4+(z_{12}-\xi^2)^2-2x_c^2\,(z_{12}+\xi^2)}\Bigg) \\
& -\ln\Bigg(-x_c^4+z_{12}\,(z_{12}-z_{123})-(z_{12}+z_{123})\,\xi^2+x_c^2\,(z_{123}+\xi^2)+ \\
& \sqrt{x_c^4+(z_{12}-z_{123})^2-2x_c^2\,(z_{12}+z_{123})}\sqrt{x_c^4+(z_{12}-\xi^2)^2-2x_c^2\,(z_{12}+\xi^2)}\Bigg)\Bigg]\Bigg] \\
& \Bigg/\Big[3\,(x_c^2-z_{12})\,z_{12}z_{123}^3\big(x_c^4+(z_{12}-z_{123})^2-2x_c^2\,(z_{12}+z_{123})\big)^2\Big],
\end{aligned}
\tag{B.6}
$$

$$
\begin{aligned}
g^{\rm r}_{cs} = & \int_{(x_c+\xi)^2}^{(1-x_c)^2} dz_{123} \int_{(x_c+\xi)^2}^{z_{123}} dz_{12} 24\,(1+x_c^2-z_{123})\,(z_{123}-z_{12}) \\
& \sqrt{x_c^4+(z_{123}-1)^2-2x_c^2\,(1+z_{123})}\Bigg[(x_c^2-z_{12})\,(x_c^2-z_{12}+z_{123}) \\
& +z_{12}\,(z_{123}-x_c^2)\Bigg[\ln\Bigg(1+\tfrac{(z_{123}-z_{12})\sqrt{x_c^4+(z_{12}-\xi^2)^2-2x_c^2(z_{12}+\xi^2)}}{(x_c^2-z_{12})(z_{12}-z_{123})+(z_{12}+z_{123})\xi^2}\Bigg) \\
& -\ln\Bigg(1-\tfrac{(z_{123}-z_{12})\sqrt{x_c^4+(z_{12}-\xi^2)^2-2x_c^2(z_{12}+\xi^2)}}{(x_c^2-z_{12})(z_{12}-z_{123})+(z_{12}+z_{123})\xi^2}\Bigg)\Bigg]\Bigg] \\
& \Bigg/\Big[(x_c^2-z_{12})\,z_{12}z_{123}\Big],
\end{aligned}
\tag{B.7}
$$

$$
\begin{aligned}
g^{\mathrm{r}}_{b\bar{c}} = & \int_{(x_c+\xi)^2}^{(1-x_c)^2} dz_{123} \int_{x_c^2}^{(\sqrt{z_{123}}-\xi)^2} dz_{12} 24 \left(x_c^2 - z_{12}\right)^2 \\
& \Bigg[\Big(1 + x_c^4 + z_{12}\left(z_{123} - 2\right) - x_c^2\left(z_{12} + z_{123} - 2\right)\Big) \ln \Bigg(z_{123}^2 + \left(x_c^2 - 1\right) \\
& \left(z_{12} - \xi^2\right) - z_{123}\left(x_c^2 + z_{12} + \xi^2 - 1\right) - \sqrt{x_c^4 + \left(z_{123} - 1\right)^2 - 2x_c^2\left(1 + z_{123}\right)} \\
& \sqrt{\left(z_{12} - z_{123}\right)^2 - 2\left(z_{12} + z_{123}\right)\xi^2 + \xi^4}\Bigg) + \tfrac{1}{z_{123}} \Bigg[- \left(z_{12} - z_{123}\right)^2 \\
& \sqrt{x_c^4 + \left(z_{123} - 1\right)^2 - 2x_c^2\left(1 + z_{123}\right)} + z_{123} \Bigg[\Big(- 1 - x_c^4 + 2x_c^2\left(z_{12} - 1\right) + z_{12} \\
& + z_{123} - z_{12} z_{123}\Big) \ln \Bigg(z_{123} + z_{12}\left(z_{123} + x_c^2 - 1\right) + \xi^2 + z_{123}\left(\xi^2 - z_{123}\right) \\
& - x_c^2\left(z_{123} + \xi^2\right) - \sqrt{x_c^4 + \left(z_{123} - 1\right)^2 - 2x_c^2\left(1 + z_{123}\right)} \\
& \sqrt{\left(z_{12} - z_{123}\right)^2 - 2\left(z_{12} + z_{123}\right)\xi^2 + \xi^4}\Bigg) - \Big(1 + x_c^4 + z_{12}\left(z_{123} - 2\right) \\
& - x_c^2\left(z_{123} + z_{12} - 2\right)\Big) \ln \Bigg(z_{12}\left(x_c^2 - 1 - z_{123}\right) + z_{123}\left(1 + z_{123} - x_c^2\right) + \xi^2 \\
& - \left(x_c^2 + z_{123}\right)\xi^2 + \sqrt{x_c^4 + \left(z_{123} - 1\right)^2 - 2x_c^2\left(1 + z_{123}\right)} \\
& \sqrt{\left(z_{12} - z_{123}\right)^2 - 2\left(z_{12} + z_{123}\right)\xi^2 + \xi^4}\Bigg) + \Big(x_c^4 - 2x_c^2\left(z_{12} - 1\right) + \left(z_{12} - 1\right) \\
& \left(z_{123} - 1\right)\Big) \ln \Bigg(z_{123} + z_{12}\left(x_c^2 + z_{123} - 1\right) + \xi^2 + z_{123}\left(\xi^2 - z_{123}\right) \\
& - x_c^2\left(z_{123} + \xi^2\right) + \sqrt{x_c^4 + \left(z_{123} - 1\right)^2 - 2x_c^2\left(1 + z_{123}\right)} \\
& \cdot \sqrt{\left(z_{12} - z_{123}\right)^2 - 2\left(z_{12} + z_{123}\right)\xi^2 + \xi^4}\Bigg)\Bigg]\Bigg]\Bigg] \Big/ \Big[z_{12}\left(z_{12} - z_{123}\right)\Big],
\end{aligned}
\tag{B.8}
$$

$$
\begin{aligned}
g^{\mathrm{r}}_{bs} = {} & \int_{4x_c^2}^{(1-\xi)^2} dz_{123} \int_{4x_c^2}^{z_{123}} dz_{12} 6\sqrt{z_{12}-4x_c^2}\,(z_{12}-z_{123}) \\
& \Bigg[\Big[z_{12}\big(z_{12}-4z_{12}^2-z_{12}z_{123}+(z_{123}-3)\,z_{123}\big)+2x_c^2\big(z_{12}+2z_{12}^2-z_{12}z_{123} \\
& +(z_{123}-3)\,z_{123}\big)\Big]\,(1-z_{123})-2\,(z_{12}-1)\,\big(-2x_c^2\,(z_{12}-1)+z_{12}\,(1+2z_{12})\big) \\
& z_{123}\Bigg[\ln\Bigg(z_{12}\Big(-1+z_{123}+\xi^2-\sqrt{(z_{123}-1)^2-2\,(1+z_{123})\,\xi^2+\xi^4}\Big) \\
& +z_{123}\Big(1-z_{123}+\xi^2+\sqrt{(z_{123}-1)^2-2\,(1+z_{123})\,\xi^2+\xi^4}\Big)\Bigg) \\
& -\ln\Bigg(z_{123}-z_{123}\Big(z_{123}-\xi^2+\sqrt{(z_{123}-1)^2-2\,(1+z_{123})\,\xi^2+\xi^4}\Big) \\
& +z_{12}\Big(z_{123}-1+\xi^2+\sqrt{(z_{123}-1)^2-2\,(1+z_{123})\,\xi^2+\xi^4}\Big)\Bigg)\Bigg]\Bigg] \\
& \Bigg/\Big[3z_{12}^{3/2}\,(z_{123}-1)\,z_{123}\Big].
\end{aligned}
\tag{B.9}
$$

Appendix C. Phase space factors for the penguin-insertion

The phase-space-integrals from the penguin insertion of Q_2 are, with $y_c = \sqrt{1-4x_c^2}$, given by:

$$
\begin{aligned}
g_{\rm PI} = -\tfrac{1}{9}\Bigg\{ & 3i\pi x_c^2\Big[-15 + 8x_c^2\left(9-20x_c^2+8x_c^4\right) + 24x_c^2\left(4x_c^2-1\right)\ln\left(4x_c^2\right)\Big] \\
& + \tfrac{1}{4y_c}\Bigg[19 - 30x_c^2 - 330x_c^4 + 476x_c^6 + 432x_c^8 + 144x_c^4 y_c\left(4+3x_c^4\right) \\
& \quad \ln\left(\tfrac{2x_c}{1+y_c}\right) + 96x_c^2 y_c\left(1+20x_c^4\right)\ln\left(\tfrac{1+y_c}{2x_c}\right)\Bigg] \\
& \quad +3\left(1-4x_c^2+36x_c^4-48x_c^6\right)\ln\left(\tfrac{-1+2x_c^2+y_c}{2x_c^2}\right) \\
& -4\Bigg[12x_c^2\ln\left(\tfrac{2x_c}{1+y_c}\right)\Bigg[1-2x_c^2\left(2+3\left(x_c^2+x_c^4\right)\right)+6x_c^2\left(x_c^4-1\right)\ln\left(\tfrac{x_c m_b}{\mu}\right)\Bigg] \\
& -\tfrac{1}{2}y_c\Bigg[1-44x_c^2+214x_c^4-36x_c^6+\left(-3+6x_c^2\left(7+x_c^2+6x_c^4\right)\right)\ln\left(\tfrac{x_c m_b}{\mu}\right)\Bigg]\Bigg] \\
& +24x_c^4\left(4x_c^2-1\right)\Bigg[\pi\left(\pi+6i\ln\left(x_c\right)\right)+6i\ln\left(\tfrac{i(1+y_c)}{2x_c}\right) \\
& \Bigg[-i\ln\left(\tfrac{i(1+y_c)}{2x_c}\right)-2i\ln\left(\tfrac{1-y_c}{2x_c^2}\right)\Bigg]-6\mathrm{Li}_2\left(-\tfrac{1-2x_c^2-y_c}{2x_c^2}\right)\Bigg]\Bigg\},
\end{aligned}
\tag{C.1}
$$

$$
\begin{aligned}
g_{\rm PI+} = -\tfrac{2x_c^2}{3}\Bigg\{ & 5y_c + x_c^2\Big[-47y_c + 2\pi^2\left(8x_c^2-1\right) + 4i\pi\left(40x_c^4-9\right) + \\
& x_c^2\big[-78y_c + 480\ln\left(2\right)^2\big] - 6\ln\left(2\right)\left(3+10\ln\left(2\right)\right)\Big] + 24x_c^2\left(-1+8x_c^2\right)\cdot \\
& \ln\left(x_c\right)\ln\left(16x_c\right) + 24x_c^2\left(8x_c^2-1\right)\ln\left(2x_c\right)\big[-\ln\left(1-y_c\right)+\ln\left(1+y_c\right)\big] \\
& +2\ln\left(\tfrac{-1+2x_c^2+y_c}{2x_c^2}\right) - 4y_c\ln\left(\tfrac{x_c m_b}{\mu}\right) + 2x_c^2\Bigg[-12i\pi\left(8x_c^2-1\right)\ln\left(2x_c\right) \\
& +6\ln\left(1+y_c\right)\left[\ln\left(\tfrac{64x_c^4}{1+y_c}\right)+8x_c^2\ln\left(\tfrac{1+y_c}{64x_c^4}\right)\right] + 9\ln\left(\tfrac{-1+2x_c^2+y_c}{x_c^2}\right) \\
& -10y_c\ln\left(\tfrac{x_c m_b}{\mu}\right) + 12x_c^2 y_c\ln\left(\tfrac{x_c m_b}{\mu}\right) + 4x_c^2\ln\left(\tfrac{1+y_c}{2x_c}\right) \\
& \left(31+12x_c^2\ln\left(\tfrac{x_c m_b}{\mu}\right)\right) + 4\ln\left(\tfrac{2x_c}{1+y_c}\right)\left[-7+39x_c^4+6\left(2x_c^2-1\right)\ln\left(\tfrac{x_c m_b}{\mu}\right)\right]\Bigg] \\
& +24x_c^2\left(1-8x_c^2\right)\mathrm{Li}_2\left(\tfrac{1}{2}\left(1-y_c\right)\right)\Bigg\}.
\end{aligned}
\tag{C.2}
$$

References

[1] A. Lenz, U. Nierste, J. Charles, S. Descotes-Genon, A. Jantsch, C. Kaufhold, H. Lacker and S. Monteil *et al.*, Phys. Rev. D **83** (2011) 036004 [arXiv:1008.1593 [hep-ph]].

[2] A. Lenz, U. Nierste, J. Charles, S. Descotes-Genon, H. Lacker, S. Monteil, V. Niess and S. T'Jampens, Phys. Rev. D **86** (2012) 033008 [arXiv:1203.0238 [hep-ph]].

[3] S. L. Glashow, Nucl. Phys. **22** (1961) 579.

[4] S. Weinberg, Phys. Rev. Lett. **19** (1967) 1264.

[5] A. Salam, Conf. Proc. C **680519** (1968) 367.

[6] N. Cabibbo, Phys. Rev. Lett. **10** (1963) 531.

[7] M. Kobayashi and T. Maskawa, Prog. Theor. Phys. **49** (1973) 652.

[8] O. Eberhardt, G. Herbert, H. Lacker, A. Lenz, A. Menzel, U. Nierste and M. Wiebusch, Phys. Rev. Lett. **109** (2012) 241802 [arXiv:1209.1101 [hep-ph]].

[9] M. Baak, M. Goebel, J. Haller, A. Hoecker, D. Kennedy, R. Kogler, K. Moenig and M. Schott *et al.*, Eur. Phys. J. C **72** (2012) 2205 [arXiv:1209.2716 [hep-ph]].

[10] F. Englert and R. Brout, Phys. Rev. Lett. **13** (1964) 321.

[11] P. W. Higgs, Phys. Rev. Lett. **13** (1964) 508.

[12] G. S. Guralnik, C. R. Hagen and T. W. B. Kibble, Phys. Rev. Lett. **13** (1964) 585.

[13] G. Aad *et al.* [ATLAS Collaboration], Phys. Lett. B **716** (2012) 1 [arXiv:1207.7214 [hep-ex]].

[14] S. Chatrchyan *et al.* [CMS Collaboration], Phys. Lett. B **716** (2012) 30 [arXiv:1207.7235 [hep-ex]].

[15] A. Djouadi and A. Lenz, Phys. Lett. B **715** (2012) 310 [arXiv:1204.1252 [hep-ph]].

[16] E. Kuflik, Y. Nir and T. Volansky, arXiv:1204.1975 [hep-ph].

[17] A. Lenz, Adv. High Energy Phys. **2013** (2013) 910275.

[18] M. A. Shifman and M. B. Voloshin, Sov. J. Nucl. Phys. **41** (1985) 120 [Yad. Fiz. **41** (1985) 187].

[19] V. A. Khoze and M. A. Shifman, Sov. Phys. Usp. **26** (1983) 387.

[20] V. A. Khoze, M. A. Shifman, N. G. Uraltsev and M. B. Voloshin, Sov. J. Nucl. Phys. **46** (1987) 112 [Yad. Fiz. **46** (1987) 181].

[21] J. Chay, H. Georgi and B. Grinstein, Phys. Lett. B **247** (1990) 399.

[22] I. I. Y. Bigi, N. G. Uraltsev and A. I. Vainshtein, Phys. Lett. B **293** (1992) 430 [Erratum-ibid. B **297** (1993) 477] [hep-ph/9207214].

[23] I. I. Y. Bigi, M. A. Shifman, N. G. Uraltsev and A. I. Vainshtein, Phys. Rev. Lett. **71** (1993) 496 [hep-ph/9304225].

[24] B. Blok, L. Koyrakh, M. A. Shifman and A. I. Vainshtein, Phys. Rev. D **49** (1994) 3356 [Erratum-ibid. D **50** (1994) 3572] [hep-ph/9307247].

[25] A. V. Manohar and M. B. Wise, Phys. Rev. D **49** (1994) 1310 [hep-ph/9308246].

[26] A. F. Falk, M. B. Wise and I. Dunietz, Phys. Rev. D **51** (1995) 1183 [hep-ph/9405346].

[27] G. Altarelli, G. Martinelli, S. Petrarca and F. Rapuano, Phys. Lett. B **382** (1996) 409 [hep-ph/9604202].

[28] I. Dunietz, J. Incandela, F. D. Snider and H. Yamamoto, Eur. Phys. J. C **1** (1998) 211 [hep-ph/9612421].

[29] R. Aleksan, A. Le Yaouanc, L. Oliver, O. Pene and J. C. Raynal, Phys. Lett. B **316** (1993) 567.

[30] C. -K. Chua, W. -S. Hou and C. -H. Shen, Phys. Rev. D **84** (2011) 074037 [arXiv:1107.4325 [hep-ph]].

[31] [LHCb Collaboration], LHCb-CONF-2012-002.

[32] R. Aaij *et al.* [LHCb Collaboration], Phys. Rev. Lett. **108** (2012) 101803 [arXiv:1112.3183 [hep-ex]].

[33] G. Aad *et al.* [ATLAS Collaboration], JHEP **1212** (2012) 072 [arXiv:1208.0572 [hep-ex]].

[34] T. Aaltonen *et al.* [CDF Collaboration], Phys. Rev. Lett. **109** (2012) 171802 [arXiv:1208.2967 [hep-ex]].

[35] V. M. Abazov *et al.* [D0 Collaboration], Phys. Rev. D **85** (2012) 032006 [arXiv:1109.3166 [hep-ex]].

[36] R. Aaij *et al.* [LHCb Collaboration], arXiv:1304.2600 [hep-ex].

[37] Y. Amhis *et al.* [Heavy Flavor Averaging Group Collaboration], arXiv:1207.1158 [hep-ex]. http://www.slac.stanford.edu/xorg/hfag/

[38] A. Lenz and U. Nierste, arXiv:1102.4274 [hep-ph].

[39] A. Lenz and U. Nierste, JHEP **0706** (2007) 072 [hep-ph/0612167].

[40] M. Beneke, G. Buchalla, A. Lenz and U. Nierste, Phys. Lett. B **576** (2003) 173 [hep-ph/0307344].

[41] M. Beneke, G. Buchalla, C. Greub, A. Lenz and U. Nierste, Nucl. Phys. B **639** (2002) 389 [hep-ph/0202106].

[42] M. Beneke, G. Buchalla, C. Greub, A. Lenz and U. Nierste, Phys. Lett. B **459** (1999) 631 [hep-ph/9808385].

[43] M. Ciuchini, E. Franco, V. Lubicz, F. Mescia and C. Tarantino, JHEP **0308** (2003) 031 [hep-ph/0308029].

[44] A. Lenz, arXiv:1205.1444 [hep-ph].

[45] A. Lenz and T. Rauh, arXiv:1305.3588 [hep-ph].

[46] D. van Dyk, talk at Beauty 2013, update of
F. Beaujean, C. Bobeth and D. van Dyk, arXiv:1301.0346 [hep-ph].

[47] W. Altmannshofer talk at Beauty 2013, update of
W. Altmannshofer and D. M. Straub, JHEP **1208** (2012) 121 [arXiv:1206.0273 [hep-ph]].

[48] S. Descotes-Genon, T. Hurth, J. Matias and J. Virto, arXiv:1305.4808 [hep-ph].

[49] RAaij *et al.* [LHCb Collaboration], Eur. Phys. J. C **73** (2013) 2373 [arXiv:1208.3355 [hep-ex]].

[50] V. M. Abazov *et al.* [D0 Collaboration], Phys. Rev. D **82** (2010) 032001 [arXiv:1005.2757 [hep-ex]].

[51] V. M. Abazov *et al.* [D0 Collaboration], Phys. Rev. Lett. **105** (2010) 081801 [arXiv:1007.0395 [hep-ex]].

[52] V. M. Abazov *et al.* [D0 Collaboration], Phys. Rev. D **84** (2011) 052007 [arXiv:1106.6308 [hep-ex]].

[53] C. Bobeth and U. Haisch, APP B **44** (2013) 127 [arXiv:1109.1826 [hep-ph]].

[54] W. Skiba and J. Kalinowski, Nucl. Phys. B **404** (1993) 3.

[55] Y. Grossman, Z. Ligeti and E. Nardi, Phys. Rev. D **55** (1997) 2768 [hep-ph/9607473].

[56] A. Dighe, A. Kundu and S. Nandi, Phys. Rev. D **82** (2010) 031502 [arXiv:1005.4051 [hep-ph]].

[57] C. W. Bauer and N. D. Dunn, Phys. Lett. B **696** (2011) 362 [arXiv:1006.1629 [hep-ph]].

[58] A. Dighe and D. Ghosh, Phys. Rev. D **86** (2012) 054023 [arXiv:1207.1324 [hep-ph]].

[59] G. Borissov and B. Hoeneisen, arXiv:1303.0175 [hep-ex].

[60] G. Altarelli and S. Petrarca, Phys. Lett. B **261** (1991) 303.

[61] I. I. Y. Bigi, B. Blok, M. A. Shifman and A. I. Vainshtein, Phys. Lett. B **323** (1994) 408 [hep-ph/9311339].

[62] A. L. Kagan, Phys. Rev. D **51** (1995) 6196 [hep-ph/9409215].

[63] E. Bagan, P. Ball, V. M. Braun and P. Gosdzinsky, Phys. Lett. B **342** (1995) 362 [Erratum-ibid. B **374** (1996) 363] [hep-ph/9409440].

[64] G. Buchalla, I. Dunietz and H. Yamamoto, Phys. Lett. B **364** (1995) 188 [hep-ph/9507437].

[65] M. Neubert and C. T. Sachrajda, Nucl. Phys. B **483** (1997) 339 [hep-ph/9603202].

[66] A. L. Kagan and J. Rathsman, hep-ph/9701300.

[67] M. Neubert, In *Jerusalem 1997, High energy physics* 243-268 [hep-ph/9801269].

[68] A. Kagan, In *Santa Barbara 1997, Heavy flavor physics* 215-243 [hep-ph/9806266].

[69] A. Lenz, hep-ph/0011258.

[70] M. B. Voloshin, Phys. Rev. D **51** (1995) 3948 [hep-ph/9409391].

[71] Y. Nir, Phys. Lett. B **221** (1989) 184.

[72] E. Bagan, P. Ball, V. M. Braun and P. Gosdzinsky, Nucl. Phys. B **432** (1994) 3 [hep-ph/9408306].

[73] E. Bagan, P. Ball, B. Fiol and P. Gosdzinsky, Phys. Lett. B **351** (1995) 546 [hep-ph/9502338].

[74] A. Lenz, U. Nierste and G. Ostermaier, Phys. Rev. D **56** (1997) 7228 [hep-ph/9706501].

[75] C. Greub and P. Liniger, Phys. Rev. D **63** (2001) 054025 [hep-ph/0009144].

[76] C. Greub and P. Liniger, Phys. Lett. B **494** (2000) 237 [hep-ph/0008071].

[77] B. Aubert *et al.* [BABAR Collaboration], Phys. Rev. D **75** (2007) 072002 [hep-ex/0606026].

[78] G. Buchalla, A. J. Buras and M. E. Lautenbacher, Rev. Mod. Phys. **68** (1996) 1125 [hep-ph/9512380].

[79] M. Gourdin and X. -Y. Pham, Nucl. Phys. B **164** (1980) 399.

[80] W. A. Bardeen, A. J. Buras, D. W. Duke and T. Muta, Phys. Rev. D **18** (1978) 3998.

[81] G. Altarelli, G. Curci, G. Martinelli and S. Petrarca, Nucl. Phys. B **187** (1981) 461.

[82] G. Buchalla, Nucl. Phys. B **391** (1993) 501.

[83] Q. Ho-kim and X. -Y. Pham, Annals Phys. **155** (1984) 202.

[84] A. J. Buras and P. H. Weisz, Nucl. Phys. B **333** (1990) 66.

[85] M. Beneke and V. M. Braun, Nucl. Phys. B **426** (1994) 301 [hep-ph/9402364].

[86] I. I. Y. Bigi, M. A. Shifman, N. G. Uraltsev and A. I. Vainshtein, Phys. Rev. D **50** (1994) 2234 [hep-ph/9402360].

[87] K. Melnikov and T. v. Ritbergen, Phys. Lett. B **482** (2000) 99 [hep-ph/9912391].

[88] I. I. Y. Bigi, M. A. Shifman, N. Uraltsev and A. I. Vainshtein, Phys. Rev. D **56** (1997) 4017 [hep-ph/9704245].

[89] M. Beneke, Phys. Lett. B **434** (1998) 115 [hep-ph/9804241].

[90] A. H. Hoang, Z. Ligeti and A. V. Manohar, Phys. Rev. Lett. **82** (1999) 277 [hep-ph/9809423].

[91] T. Hahn and M. Perez-Victoria, Comput. Phys. Commun. **118** (1999) 153 [hep-ph/9807565].

[92] J. Beringer *et al.* [Particle Data Group Collaboration], Phys. Rev. D **86** (2012) 010001.

[93] S. Alekhin, J. Blmlein, K. Daum, K. Lipka and S. Moch, Phys. Lett. B **720** (2013) 172 [arXiv:1212.2355 [hep-ph]].

[94] C. McNeile, C. T. H. Davies, E. Follana, K. Hornbostel and G. P. Lepage, Phys. Rev. D **82** (2010) 034512 [arXiv:1004.4285 [hep-lat]].

[95] K. G. Chetyrkin, J. H. Kuhn, A. Maier, P. Maierhofer, P. Marquard, M. Steinhauser and C. Sturm, Phys. Rev. D **80** (2009) 074010 [arXiv:0907.2110 [hep-ph]].

[96] B. Dehnadi, A. H. Hoang, V. Mateu and S. M. Zebarjad, arXiv:1102.2264 [hep-ph].

[97] A. Kagan, F. Krinner, A. Lenz, U. Nierste and T. Rauh in prep.